

Probabilistic seismic hazard assessment for sliding displacement of slopes: an application in Turkey

Zeynep Gülerce¹ · Onur Balal²

Received: 21 January 2016 / Accepted: 23 December 2016 / Published online: 31 December 2016
© Springer Science+Business Media Dordrecht 2016

Abstract Earthquake-induced slope instability is one of the major sources of earthquake hazards in near fault regions. Simplified tools such as Newmark's sliding block (NSB) analysis are widely used to estimate the sliding displacement of slopes during earthquake shaking. Additionally, empirical models for predicting NSB displacement using single or multiple ground motion intensity measures based on global (e.g. NGA-W1 database, Chiou et al. 2008) or regional datasets are available. The objective of this study is to evaluate the compatibility of candidate NSB displacement prediction models for the probabilistic seismic hazard assessment (PSHA) applications in Turkey using a comprehensive dataset of ground motions recorded during the earthquakes occurred in Turkey. Then, application of the most suitable NSB displacement prediction model in the vector-valued PSHA framework is demonstrated using the seismic source characterization models developed for Bolu-Gerede Region (in northwest Turkey). The results are presented in terms of the NSB displacement hazard curves and the hazard curves are evaluated for the influence of parameter selection (site conditions, yield acceleration, distance to the fault plane, and other seismic source model parameters) on the final hazard output.

Keywords Earthquake-induced slope instability · Newmark's sliding block analysis · Probabilistic seismic hazard assessment · Ground motion prediction models · Landslide susceptibility

✉ Zeynep Gülerce
zyilmaz@metu.edu.tr

¹ Civil Engineering Department K1-308, Middle East Technical University, 06800 Ankara, Turkey

² Directorate General of Foundations, Ankara, Turkey

1 Introduction

Earthquake-induced slope instability is considered as one of the most important hazards related to ground shaking, especially in the near fault regions. Many earthquake scientists had made the effort to assess the landslide hazards and/or produced susceptibility maps portraying the spatial distribution of landslide-related hazards. According to Süzen and Doyuran (2004), basic conceptual model for landslide hazard mapping includes; (1) mapping a set of geological-geomorphological factors that are directly or indirectly correlated with slope instability, (2) estimating the relative contribution of these factors in generating a slope failure, and (3) classification of land surface into zones of different susceptibility degrees. Only earthquake-related parameter in this conceptual model is the distance to the fault plane. Therefore, traditional landslide susceptibility mapping approach misses the important features of planar seismic source characterization models such as the relative rate of different magnitude events, activity rate, slip rate and seismic moment accumulation, etc. Additionally, the ground motion variability represented in the ground motion characterization models is not considered. In order to integrate the earthquake-induced landslide hazard in regional or event-specific hazard and loss estimates, a complete probabilistic seismic hazard assessment (PSHA) framework that includes all of these components should be utilized.

Simplified tools like Newmark's sliding block (NSB) analogy are widely used to represent the performance of shallow slides during ground shaking since the outcome of this analogy is quantitative and appropriate for hazard-based assessment procedures: larger NSB displacement values indicate higher seismic slope instability hazard. On the other hand, NSB analogy requires extensive computational efforts in large-scaled and regional applications. The NSB displacement prediction models avoid the obstacle of selecting suitable input time histories and extensive calculations by estimating the NSB displacement based on ground motion intensity measures (IMs) and links the earthquake scenarios to the earthquake-induced landslide hazard in the PSHA context. Recently, empirical predictive models for rigid-block NSB displacement based on global ground motion datasets (mainly the subsets of PEER NGA-W1 database by Chiou et al. 2008) were proposed by Watson-Lamprey and Abrahamson (2006), Jibson (2007), Bray and Trava-sarou (2007), and Saygılı and Rathje (2008). These models work in a similar way to ground motion prediction equations (GMPEs) such that the NSB displacement is predicted as a function of the given ground motion IMs (Rathje and Saygılı 2008). Therefore, performance and applicability of the NSB prediction model in the target region should be carefully analyzed.

The primary objective of this study is to evaluate the compatibility of global NSB displacement prediction models for the PSHA applications in Turkey using a comprehensive dataset of Turkish ground motions (Gülerce et al. 2016). In addition to the global models, a regional NSB displacement prediction model developed by Bozbey and Gündoğdu (2011) based on Turkish strong motion records, Hsieh and Lee (2011) model that includes a large number of strong motions from Kocaeli (1999) and Düzce (1999) earthquakes, and a recently developed prediction model based on the numerical analysis of two-dimensional slopes by Fotopoulou and Pitilakis (2015) are included in the candidate model list. Performance of the candidate NSB displacement prediction models are evaluated using the analysis of residuals. Details regarding the candidate NSB displacement models and their compatibility with the NSB displacements in the Turkish strong motion dataset are elaborated in the next two sections.

Rathje and Saygılı (2008) documented the scalar and vector-valued PSHA structure for NSB displacement where the outcome is the annual rate of exceedance for particular NSB displacement values (in other words *the hazard curve* for NSB displacement). However, application of the defined methodology in regional-scale is not yet fully addressed (except for two examples for Southern California and Anchorage by Saygılı and Rathje 2009 and Wang and Rathje 2015) mainly because estimating the yield acceleration (a_y) for large areas based on topographical, geological and geotechnical factors is a challenging issue and the vector-valued PSHA analyses are time-consuming since these algorithms are currently not very efficient. In the second part of this manuscript, the application of the selected NSB displacement prediction model in the vector-valued PSHA framework is demonstrated in terms of the hazard integral and its main components. Bolu-Gerede Region (located in northwest Turkey) is selected as the application area since damaging earthquake-induced landslides were reported in this region after the 1999 Kocaeli and Düzce earthquakes. Sensitivity analyses are performed to understand and discuss the influence of different input parameters (e.g. site conditions, yield acceleration, distance to the fault plane, and other seismic source model parameters) on the final hazard output. Results presented here intend to argue the existing gaps in the current state-of-the-art of estimating the earthquake induced landslide hazard in a probabilistic manner and points out the direction for the future research in this field.

2 Candidate predictive models for NSB displacement

Methods for modeling and predicting the slope displacements during earthquakes have been evolving steadily since Newmark (1965) first introduced a simple model to estimate the co-seismic slope displacement. One of the earlier predictive models for the NSB displacement (D_n) was proposed by Ambraseys and Menu (1988) where D_n was modelled as a function of the critical acceleration ratio (a_c/PGA) based on the analysis of 50 strong motion records. Later on, empirical models in different functional forms have been proposed by Yegian et al. (1991), Jibson (1993), Ambraseys and Srbulov (1994, 1995), and Crespellani et al. (1998) with various additional parameters included to estimate D_n . These models were developed based on limited datasets and the resulting predictive equations displayed very large variabilities. Jibson et al. (1998) modified the functional form of the Jibson (1993) model using logarithmic terms and enlarged the size of the database tremendously (to 555 strong-motion records from 13 earthquakes) which eventually increased the aleatory variability of the predictions. In his recent work, Jibson (2007) handled this increase in the variability by adding other parameters to the prediction model as well as compiling a more comprehensive dataset (a collection of 2270 strong-motion records from 30 worldwide earthquakes). Variety of regression models with different functional forms for different ground motion IMs such as peak ground acceleration (PGA or a_{max}) and Arias intensity (I_a) were proposed by Jibson (2007). Jibson (2007) mentioned that I_a is superior to PGA in characterizing the shaking content of an earthquake record since it accounts for all acceleration peaks and for duration; therefore, the models that include I_a are physically stronger. In this study, we tested the following NSB prediction equation proposed by Jibson (2007) considering that it has the smallest standard deviation compared to other alternatives:

$$\log D_n = 0.561 \log I_a - 3.833 \log(a_c/a_{max}) - 1.474 \pm 0.616 \quad (1)$$

The NSB displacement prediction model proposed by Watson-Lamprey and Abrahamson (2006) was derived using the PEER NGA-W1 database that contains 3079 ground motion pairs (of two horizontal components) from 175 earthquakes. These 6158 recordings were scaled by seven different scale factors (0.5, 1, 2, 4, 8, 16 and 20) and the NSB displacements of these scaled recordings were computed for three yield accelerations (0.1, 0.2 and 0.3 g). The set of NSB displacements were fit to Eq. (2) using least squares regression:

$$\begin{aligned} \ln D_n = & 5.47 + 0.451((\ln(Sa_{T=1}) - 0.45) + 0.0186((\ln(Sa_{T=1}) - 0.45))^2 \\ & + 0.596((\ln(A_{RMS}) - 1)) + 0.656\left(\ln\left(\frac{Sa_{T=1}}{PGA}\right)\right) \\ & - 0.0716\left(\ln\left(\frac{Sa_{T=1}}{PGA}\right)\right)^2 + 0.802(\ln(Dur_{ky}) - 0.74) \\ & + 0.0763(\ln(Dur_{ky}) - 0.74)^2 + \frac{1}{-0.581\left(\ln\left(\frac{PGA}{k_y}\right) + 0.193\right)} \end{aligned} \quad (2)$$

where $Sa_{T=1s}$ is spectral acceleration with 5% damping at 1 s spectral period in g, A_{RMS} is the root mean square of acceleration in g, k_y is the yield acceleration in g, and Dur_{ky} is the duration for which the acceleration is greater than the yield acceleration in seconds.

Bray and Travarasou (2007) also used the PEER NGA-W1 database; however, the ground motions from large-to-moderate magnitude events recorded within 100 km rupture distance on NEHRP B, C, or D sites were selected (a total number of 688 records from 41 earthquakes). Bray and Travarasou (2007) employed one ground motion IM (PGA) and one earthquake parameter (M_w , moment magnitude) in the prediction model for the Newmark rigid sliding block case as shown in Eq. (3). The M_w term in the prediction model shows that the NSB displacement still has a conditional dependency on the earthquake scenario and the employed IM is not fully *sufficient*. Sufficiency of an IM is desirable, because it reduces the complexity in the probabilistic seismic demand analysis as well as the record selection procedure (Luco and Cornell 2007). If an insufficient IM is used and the selected records do not represent the hazard at the site, the performance-based seismic evaluation will be biased (Tothong and Cornell 2006).

$$\begin{aligned} \ln(D_n) = & -0.22 - 2.83\ln(k_y) - 0.333(\ln(k_y))^2 + 0.566\ln(k_y)\ln(PGA) \\ & + 3.04\ln(PGA) - 0.244(\ln(PGA))^2 + 0.278(M - 7) \end{aligned} \quad (3)$$

Saygılı and Rathje (2008) proposed both scalar and vector-valued models in an effort to reduce the standard deviation of the NSB displacement prediction model. Their subset of PEER NGA-W1 database includes the ground motions from earthquakes ranging from $5 < M_w < 7.9$ and the rupture distances from 0.1 to 100 km. Ground motions recorded on soft sites, or with high-pass filter corner frequencies larger than 0.25 Hz, or low-pass filter corner frequencies less than 10 Hz were removed, resulting in a dataset including 2383 ground motions. Approximately 25% of the initial ground motion dataset had PGA values of less than 0.05 g which is the minimum a_y value used in the analyses; therefore, these motions did not result in a positive NSB displacement. To further populate the dataset at larger values of PGA, NSB displacements were also calculated for each ground motion scaled by factors of 2.0 and 3.0, but the ground motions were capped at $PGA = 1.0$ g to ensure that unreasonable PGA values were not created. Computed displacement values were used to develop prediction equations as a function of k_y and different combinations of

ground motion IMs (PGA, PGV, mean period, I_a). Saygılı and Rathje (2008) proposed the generalized predictive model shown below:

$$\ln(D_n) = a_1 + a_2 \left(\frac{k_y}{\text{PGA}} \right) + a_3 \left(\frac{k_y}{\text{PGA}} \right)^2 + a_4 \left(\frac{k_y}{\text{PGA}} \right)^3 + a_5 \left(\frac{k_y}{\text{PGA}} \right)^4 + a_6 \ln(\text{PGA}) + a_7 \ln(\text{GM2}) + a_8 \ln(\text{GM3}) \quad (4)$$

where GM2 and GM3 are the ground motion parameters included in addition to PGA. For the scalar model, both GM terms were not utilized and for the two-IM models, the GM3 term was cancelled. Based on their ability to significantly reduce the standard deviation for the NSB displacement prediction, the two-IM vector-valued model (PGA, PGV) and the three-IM vector-valued model (PGA, PGV, I_a) were recommended by the authors (also considered in this study).

Bozbey and Gündoğdu (2011) developed empirical NSB displacement prediction model using a dataset compiled by Earthquake Department of General Directorate of Disaster Affairs of Turkey (AFAD) with 50 strong-motions recorded during 37 earthquakes. In this regional model, permanent slope displacements due to seismic loading were calculated for positive and negative polarities; therefore, 4 separate analyses are conducted for each recording for a_y/a_{\max} values ranging from 0.01 to 0.9. The functional form of the model is given below:

$$\log(D_n) = -4.39(a_y/a_{\max}) + 1.94 \quad (5)$$

An empirical NSB displacement prediction model for Taiwan was proposed by Hsieh and Lee (2011) based on strong motions recorded during 1999 Chi–Chi earthquake (373 strong-motion records from the Chi–Chi mainshock), 1999 Kocaeli earthquake (41 records), 1999 Düzce earthquake (20 records), 1995 Kobe earthquake, 1994 Northridge earthquake, and 1989 Loma Prieta earthquake. The parameters used in the prediction model (I_a and a_c) were similar to the model proposed by Jibson (2007); however, local site conditions were also considered and separate prediction models for rock and soil conditions were proposed. The authors suggested the use of rock-site model in regional earthquake-induced landslide hazard assessment since most natural slope failures occur on hillsides, which usually lay at the top of the bedrock; therefore, Eq. (6) is chosen to be the representative prediction equation for this study.

$$\log(D_n) = 0.788 \log(I_a) - 10.166(a_c) + 5.95a_c \log(I_a) + 1.77 \pm 0.294 \quad (6)$$

Fotopoulou and Pitilakis (2015) developed scalar and vector-valued slope displacement prediction models based on two dimensional, fully non-linear numerical analyses performed for idealized step-like slope configurations by employing 40 ground motions recorded on rock outcrop taken from the SHARE database (Seismic Hazard Harmonization in Europe, www.share-eu.org) as input motion. Considering that the vector-valued prediction models have the smallest standard deviations (or more efficient), Eq. (7) proposed by Fotopoulou and Pitilakis (2015) is tested in this study:

$$\ln(D_n) = -8.076 + 1.873 \ln(\text{PGV}) + 0.2 \ln(I_a) - 5.964(k_y) \pm 0.61 \quad (7)$$

3 Applicability of candidate NSB displacement predictive models for PSHA analyses in turkey

Implementation of global GMPEs, especially the NGA-W1 models developed mainly for California in the other shallow crustal and active tectonic regions is a topic of ongoing discussion (Stafford et al. 2008; Scasserra et al. 2009; Shoja-Taheri et al. 2010; Bradley 2013). Gülerce et al. (2016) modified and used the Turkish Strong Motion Database (Akkar et al. 2010) to check the compatibility of the magnitude, distance, and site amplification scaling of NGA-W1 horizontal prediction models with the ground motions recorded in Turkey. Analysis results showed that the horizontal NGA-W1 GMPEs overestimate the ground motions from the earthquakes occurred in Turkey, especially for the small magnitude events and for the recordings on stiff soil-rock sites. Consequently, the NSB displacement predictive models based on the global datasets should be evaluated before being implemented in PSHA studies conducted in Turkey.

Unfortunately, the Turkish strong motion database compiled for Gülerce et al. (2016) study cannot be directly used in the evaluation of NSB prediction models since the NSB displacements were not included. We calculated the NSB displacements for several values of a_y varying in between 0.02 and 0.40 g without scaling the ground motions in the dataset. NSB displacements for the given a_y are calculated for both horizontal components of each ground motion in the dataset. For each horizontal component, displacements are calculated for both positive and negative polarities (by flipping the time history upside down), and the largest displacement is assigned as the NSB displacement for that particular horizontal component in the dataset.

The Turkish strong motion dataset used by Gülerce et al. (2016) includes 1142 recordings from 288 events; however, the number of ground motion recordings with PGA values bigger than the lowest a_y is limited to 220 for the horizontal component motions in the N-S direction and 213 for the horizontal component motions in the E-W direction. According to Fig. 1a, almost 80% of the recordings in the Turkish strong motion dataset have a PGA value less than 0.1 g. Both N-S and E-W components of 190 recordings have PGA values over 0.02 g, therefore, the total number of recordings giving non-zero NSB displacements in the Gülerce et al. (2016) dataset is 243 for the smallest a_y value. Distribution of the recordings giving non-zero NSB displacement with respect to a_y is shown in Fig. 1c.

Distribution of the recordings in the magnitude-distance space (Fig. 1b) shows that the recordings obtained from events with magnitudes of 6.0 and above and the recordings from the moderate-to-large magnitude events within 30 km from the rupture are rather sparse. Almost half of the strong ground motion records included in the dataset have a moment magnitude value in between 4.5 and 5.5. Moreover, 1999 Kocaeli and Düzce earthquakes are the only events in the dataset with magnitude greater than 7.0. Even if the dataset used in this study is relatively larger than the dataset of the only regional model proposed by Bozbey and Gündoğdu (2011), it is still significantly smaller than the datasets of global models, especially in the moderate-to-large magnitude range. Therefore, any NSB displacement prediction model that will be developed from this dataset may suffer from the statistical instability in the large magnitude-short distance range. However, this dataset can be used to evaluate the applicability of the candidate models for PSHA analysis to be conducted in Turkey.

The preferred methodology for evaluating the differences between the model predictions and the calculated NSB displacements is the analysis of model residuals. The model

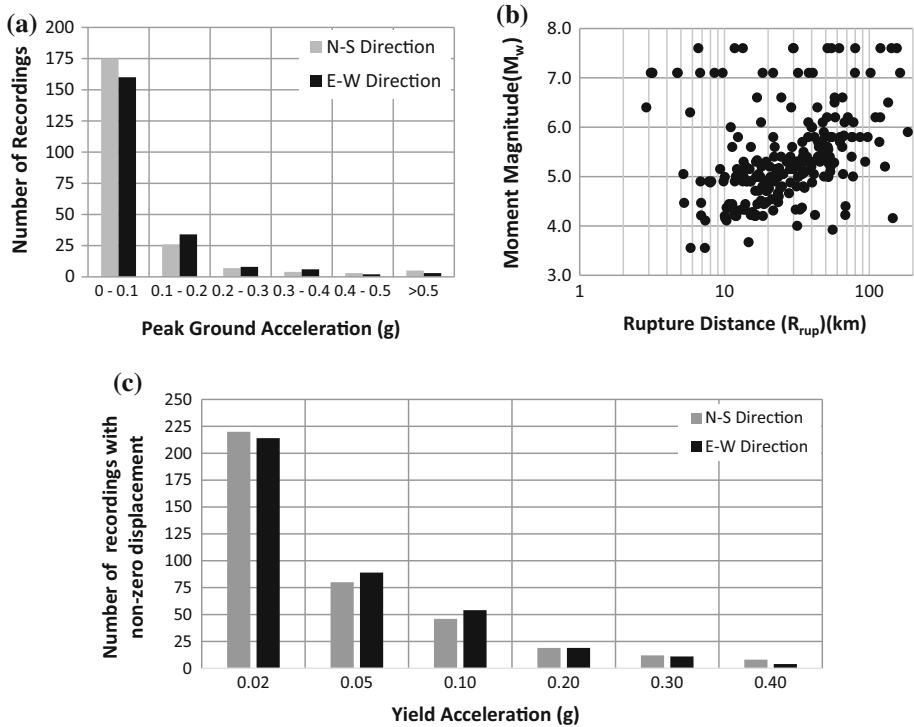


Fig. 1 **a** Distribution of the ground motions in N-S and E-W directions with respect to PGA, **b** magnitude-distance distribution of recordings that gives non-zero NSB displacements for the smallest yield acceleration value, **c** distribution of the horizontal components that gives non-zero NSB displacements for each yield acceleration value (please note that only the analysis with $a_y = 0.02$ g is used in model testing procedure)

residual is calculated by Eq. (8) for Jibson (2007), Bozbey and Gündoğdu (2011), and Hsieh and Lee (2011) models and by Eq. (9) for the other candidate models:

$$\text{Residual} = \log(\text{calculated}) - \log(\text{predicted}) \tag{8}$$

$$\text{Residual} = \ln(\text{calculated}) - \ln(\text{predicted}) \tag{9}$$

where $\ln(\text{calculated})$ and $\log(\text{calculated})$ are the NSB displacement for one of the horizontal components of the recording and $\ln(\text{predicted})$ and $\log(\text{predicted})$ are the model prediction in natural log terms or log terms. Plots of the total residuals with respect to several ground motion IMs (included in the predictive model or employed by other models) are prepared to evaluate the systematic differences between the NSB displacement values in the Turkish strong motion dataset and model predictions (Figs. 2, 3, 4, 5, 6, 7, 8, 9).

The residuals plots of the NSB displacement prediction model proposed by Watson-Lamprey and Abrahamson (2006) with respect to PGA/k_y , I_a , PGA , PGV , $Sa_{T=1s}$, $Sa_{T=1s}/PGA$, A_{RMS} , and duration are given in Fig. 2a–h, respectively. No trends in the residuals are observed in Fig. 2a–d, g. However, a constant shift along the zero line is visible in all of these plots, indicating that the constant term of the model (5.47 in Eq. 2) should be modified according to the strong motion dataset of Turkey. Figure 2e, f show that the

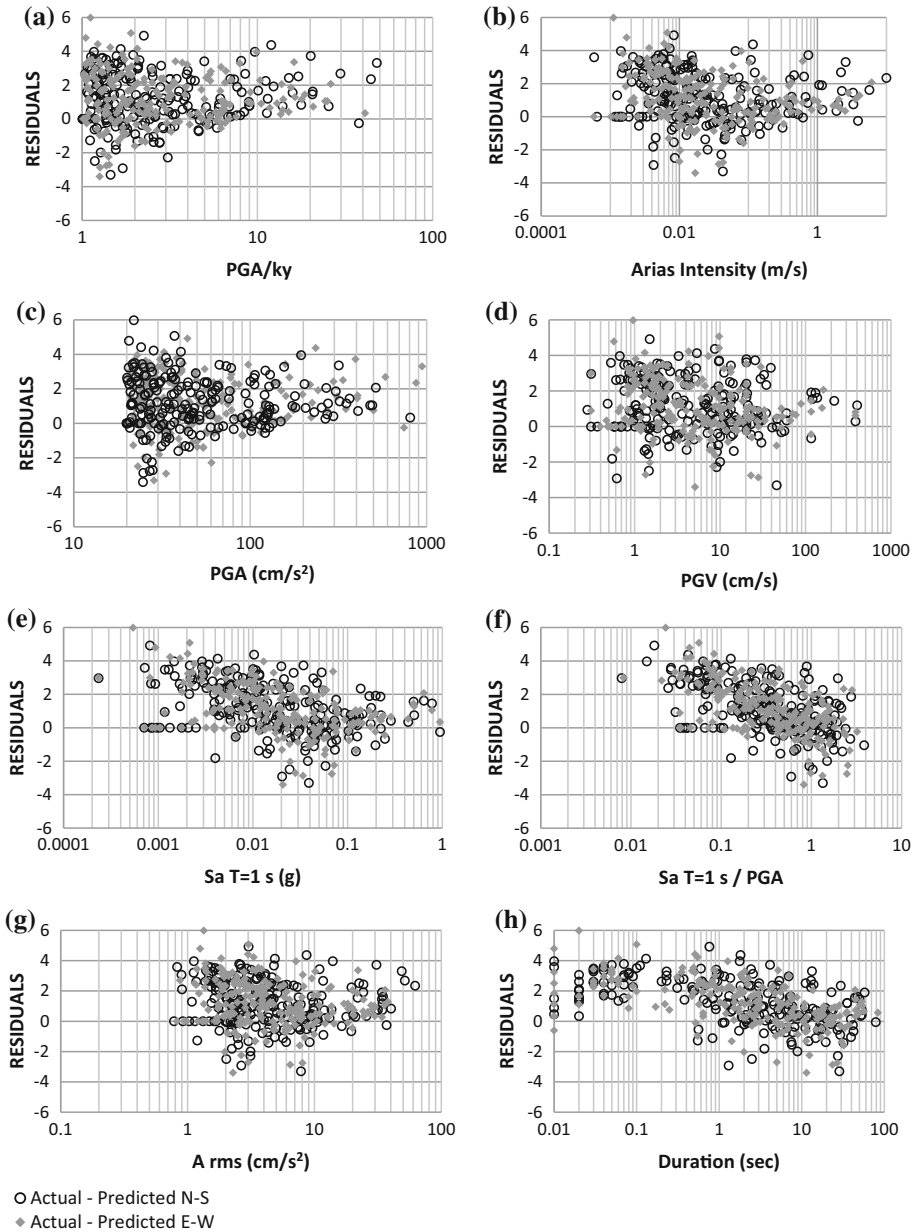


Fig. 2 Residuals of Watson-Lamprey and Abrahamson (2006) model versus **a** PGA/ k_y , **b** Arias intensity, **c** PGA, **d** PGV, **e** S_a at $T = 1$ s, **f** S_a at $T = 1$ s/PGA, **g** A_{rms} and **h** duration for $a_y = 0.02$ g

prediction model underestimates the actual NSB displacements, especially for the small spectral accelerations. This result is expected since the NGA-W1 models for the horizontal ground motion component significantly overestimates the ground motions in the Turkish comparison dataset (especially for small-to-moderate magnitudes) and this feature of the

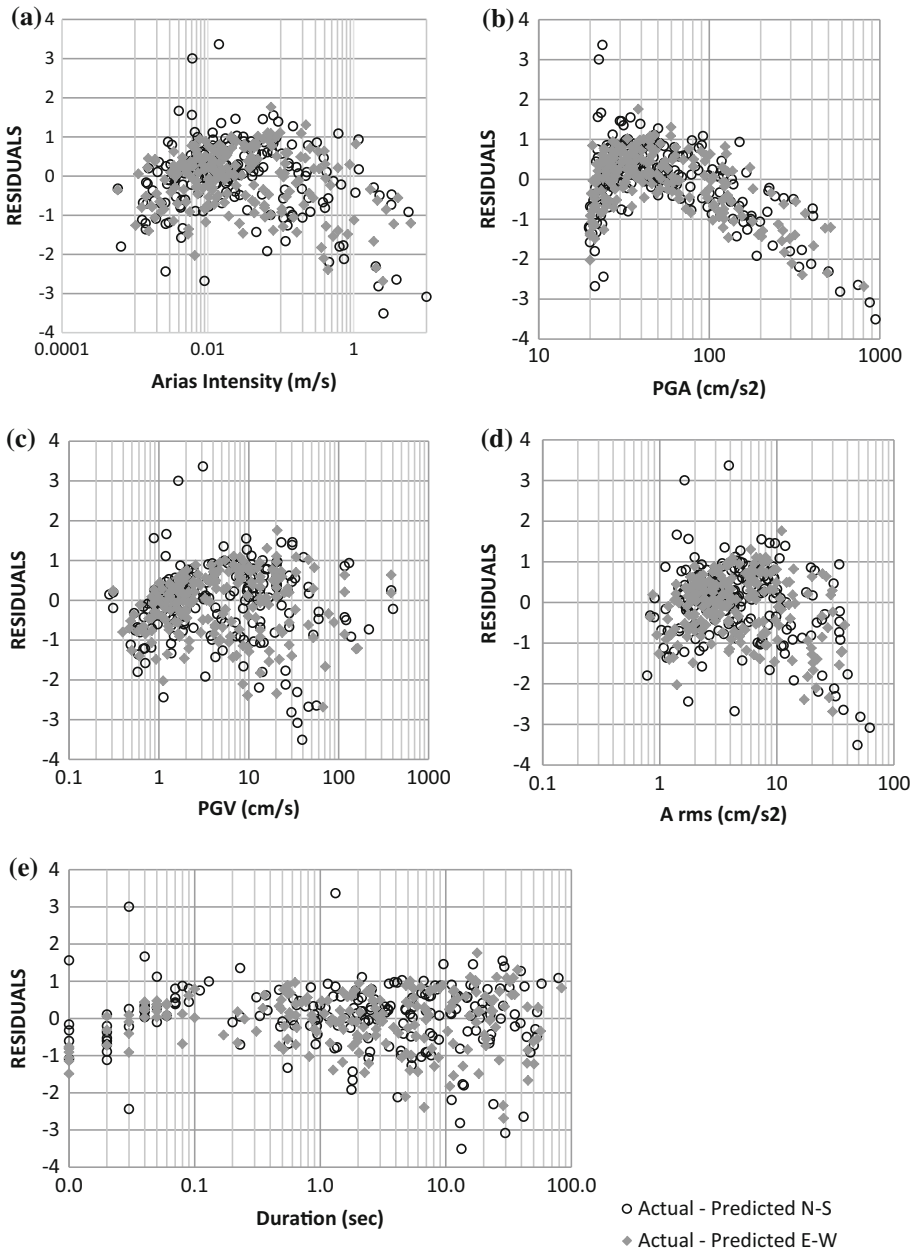


Fig. 3 Residuals of Jibson (2007) model versus **a** Arias intensity, **b** PGA, **c** PGV, **d** A_{rms} , and **e** duration for $a_y = 0.02$ g

NGA-W1 models had to be adjusted by Gülerce et al. (2016). A similar adjustment may be applied to Watson-Lamprey and Abrahamson (2006) model, however, the dataset used in this study is quite small (only 243 ground motions); therefore, the results may not be very reliable. A similar trend in the residuals is observed in distribution of residuals with respect

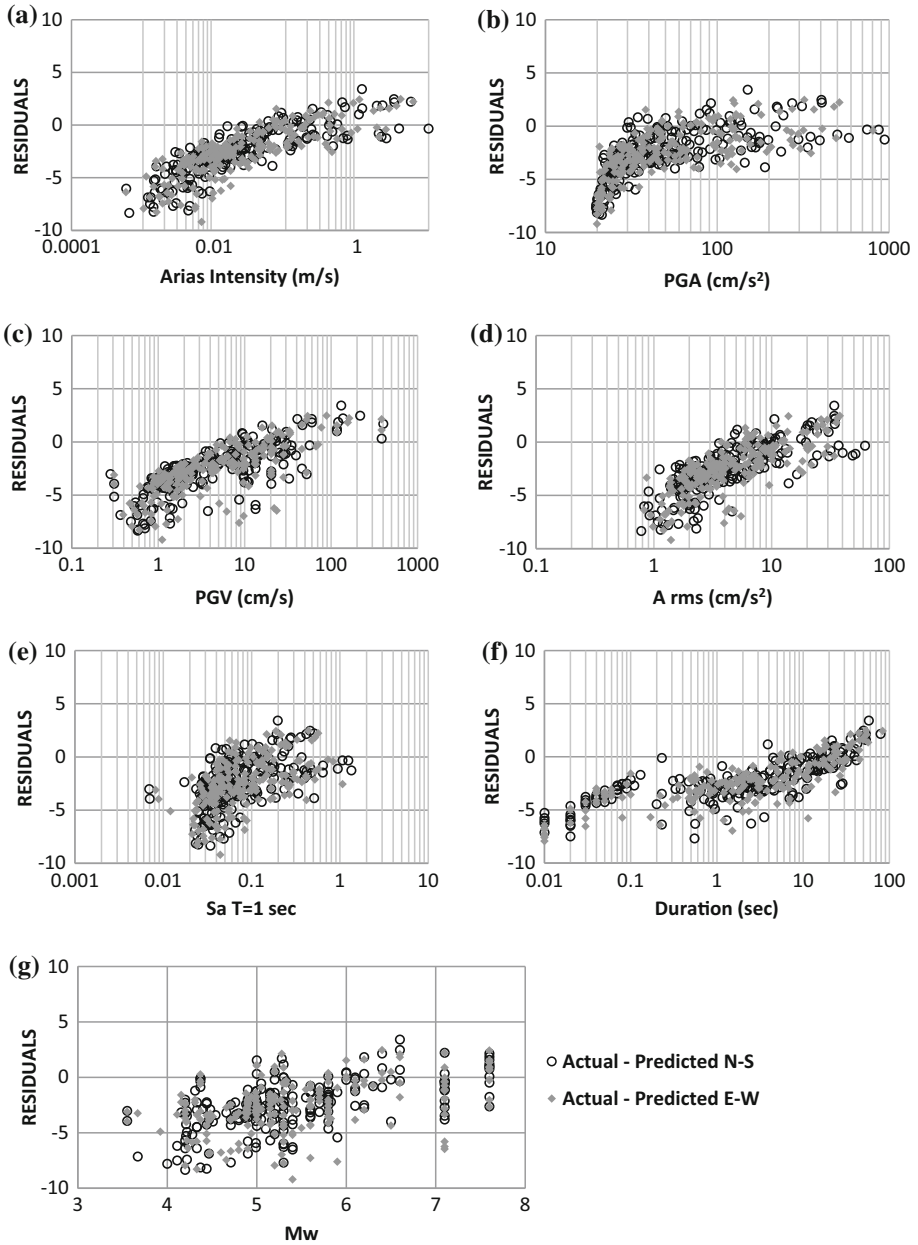


Fig. 4 Residuals of Bray and Travararou (2007) model versus **a** Arias intensity, **b** PGA, **c** PGV, **d** A_{rms} , **e** S_a at $T = 1$ s, **f** duration, and **g** M_w for $a_y = 0.02$ g

to duration (Fig. 2h) which could be related to the differences in the definition of duration in the Watson-Lamprey and Abrahamson (2006) model and in our dataset.

Residuals of the Jibson (2007) NSB displacement prediction model are plotted with respect to different ground motion parameters: I_a and PGA (included in the model), PGV,

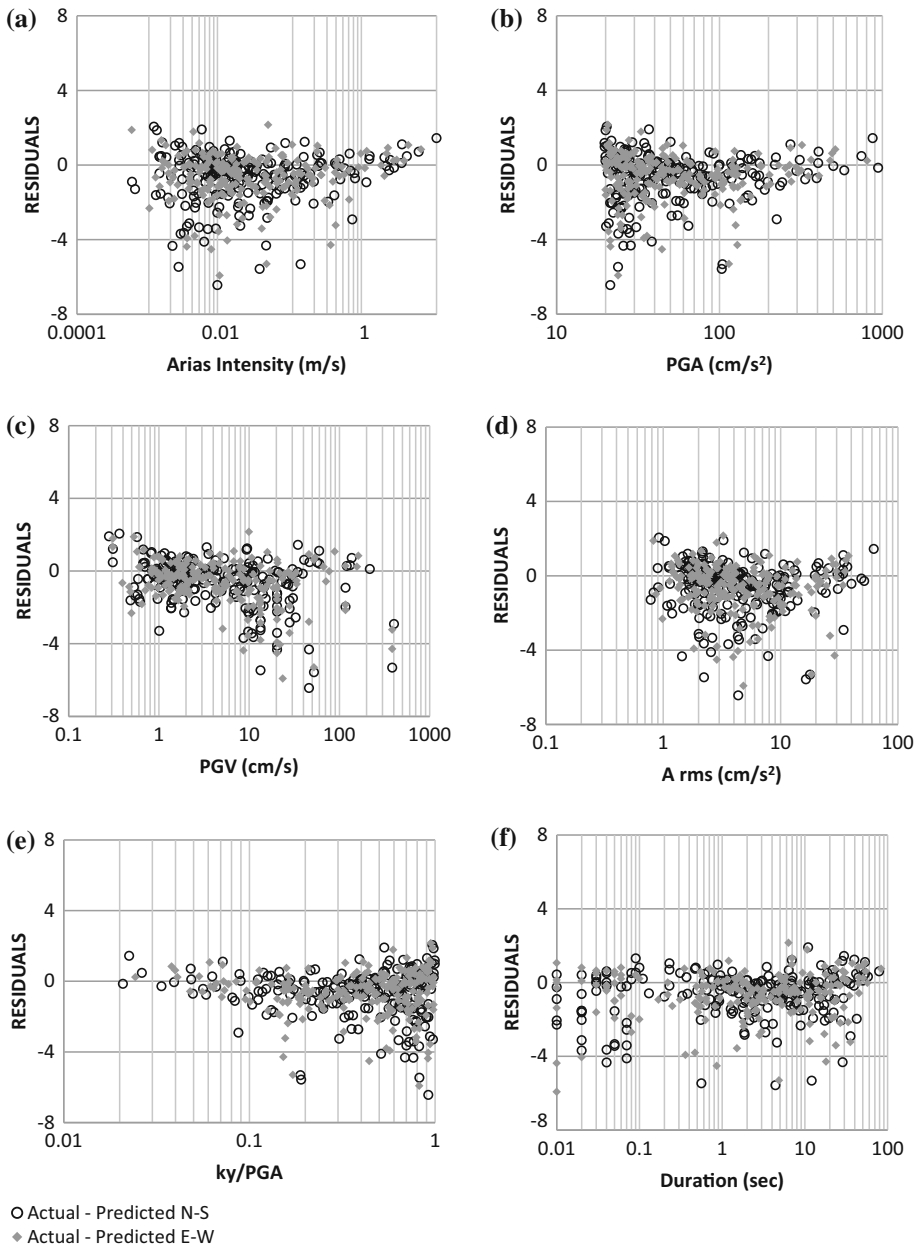


Fig. 5 Residuals of two-IM vector model (PGA, PGV) of Saygili and Rathje (2008) versus **a** Arias intensity, **b** PGA, **c** PGV, **d** A_{rms} , **e** k_y/PGA , and **f** duration for $a_y = 0.02$ g

A_{RMS} and duration (not included in the model) in Fig. 3a–e, respectively. Trends in the residual plots are not significant for I_a , PGV, A_{rms} , and duration. When compared to the Watson-Lamprey and Abrahamson (2006) model, the trend in the plot of residuals with

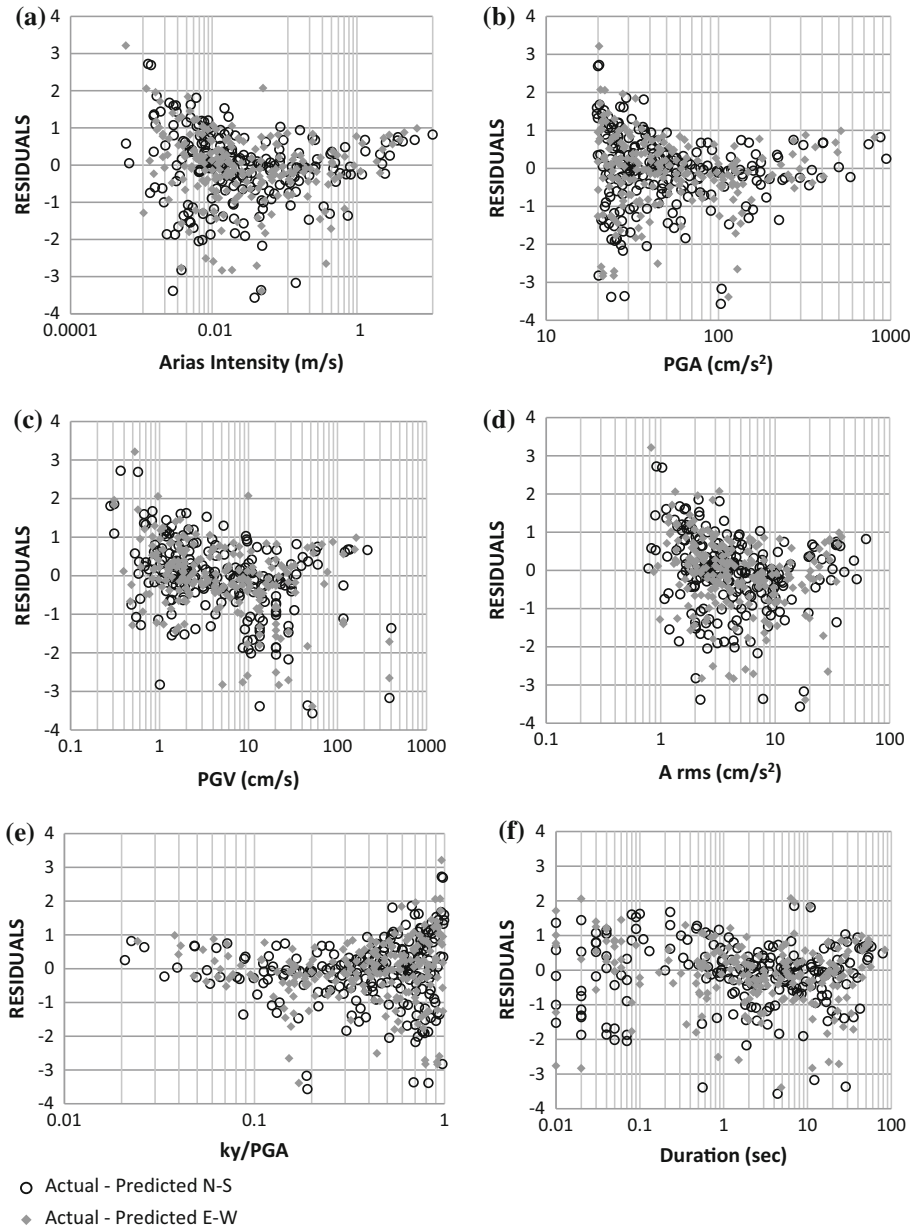


Fig. 6 Residuals of three-IM vector model (PGA, PGV, I_a) of Saygılı and Rathje (2008) versus **a** Arias intensity, **b** PGA, **c** PGV, **d** A_{rms} , **e** k_y/PGA and **f** duration for $a_y = 0.02$ g

respect to PGA is more visible; indicating that the quadratic term in the Watson-Lamprey and Abrahamson (2006) model has a positive influence on the model performance.

Figure 4 evaluates the compatibility of the Bray and Travararou (2007) model with the Turkish ground motion dataset by plotting the residuals with respect to I_a , PGA, PGV, A_{RMS} , $Sa_{T=1s}$, duration and M_w . Significant trends are observed in all of these plots

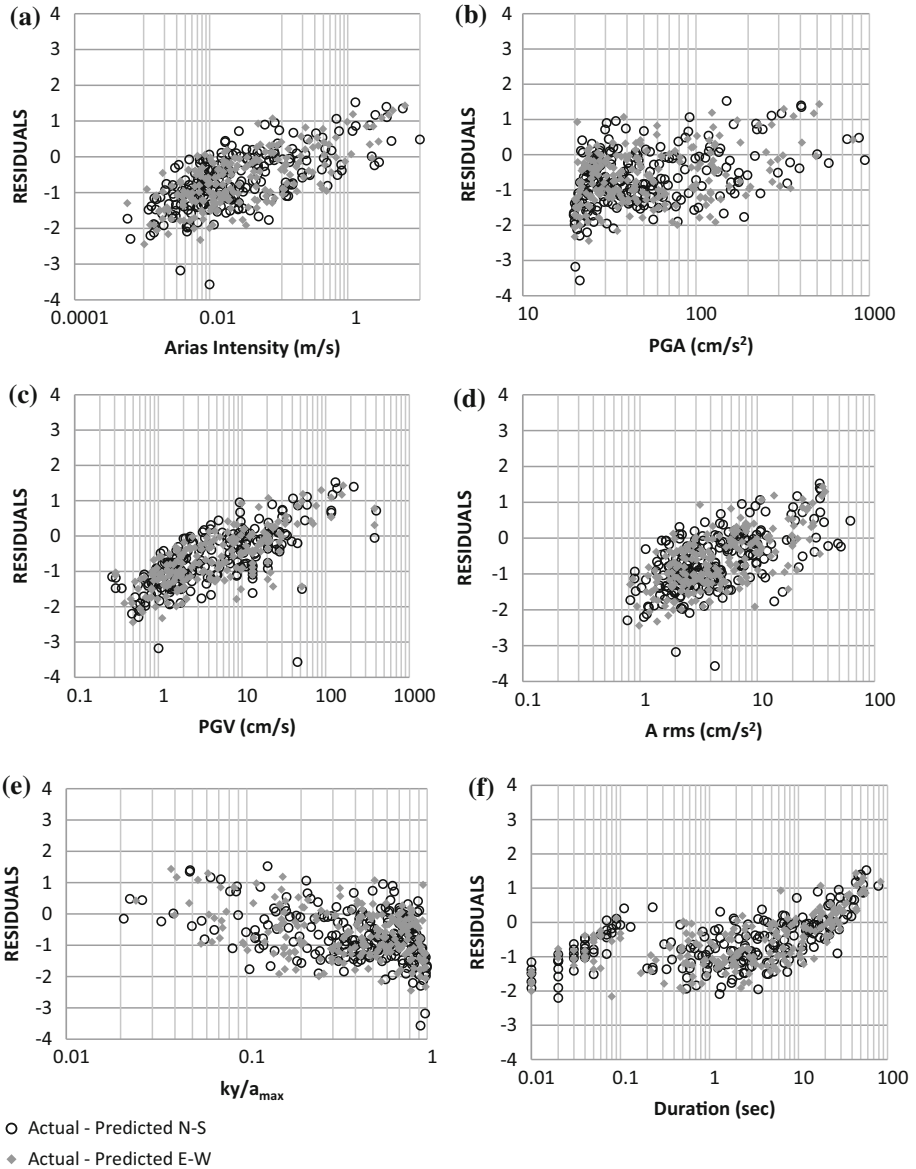


Fig. 7 Residuals of Bozbey and Gündoğdu (2011) model versus **a** Arias intensity, **b** PGA, **c** PGV, **d** A_{rms} , **e** ky/a_{max} and **f** duration at $a_y = 0.02$ g

revealing that the model is biased extensively in predicting the calculated NSB displacements for the ground motions in Turkish dataset, especially for small magnitudes and at small ground shaking levels. It is noteworthy that a significant portion of this misfit comes from the recommended cut-off value for the application of the model. Bray and Travarou (2007) mentioned that when the median NSB displacement is less than 1 cm (as most of the data in our dataset), the prediction model assumes that the displacement is equal to zero

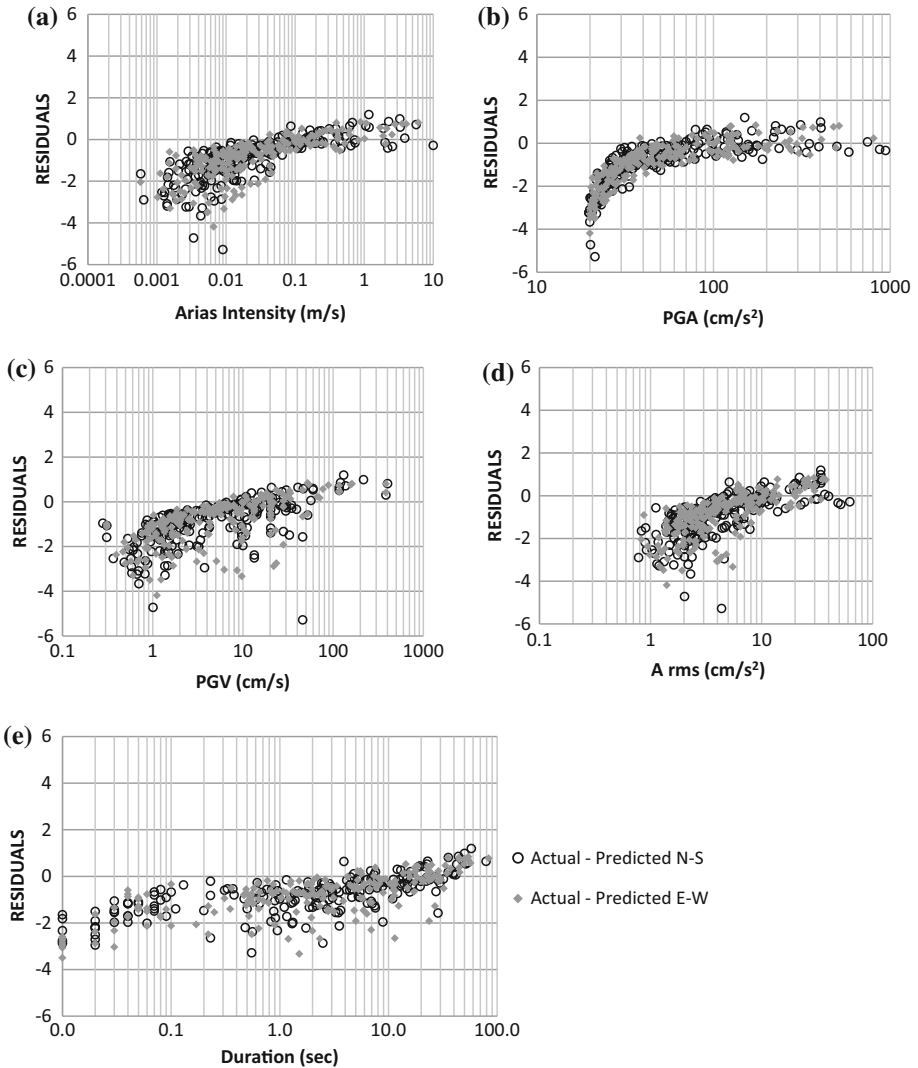


Fig. 8 Residuals of Hsieh and Lee (2011) model versus **a** Arias intensity, **b** PGA, **c** PGV, **d** A_{rms} and **e** duration at $a_y = 0.02$ g

since displacements smaller than 1 cm are not of engineering significance. Figure 4b, g indicate that the functional form of the model given in Eq. (3) should be revised for applicability in Turkey. Additionally, Fig. 4a, d, f imply that the model is unable to capture the ground motion properties represented by I_a , duration, or A_{RMS} and any one of those parameters may be included in the model for better performance.

Both two-IM (including PGA, PGV) and three-IM (including PGA, PGV, I_a) vector-valued models proposed by Saygılı and Rathje (2008) are considered as candidate models and their performance on predicting the calculated NSB displacements are evaluated by the residual plots. The residual plots of the two-IM vector-valued model with respect to I_a , PGA, PGV, A_{RMS} , k_y/PGA and duration are presented in Fig. 5a–f, respectively. No

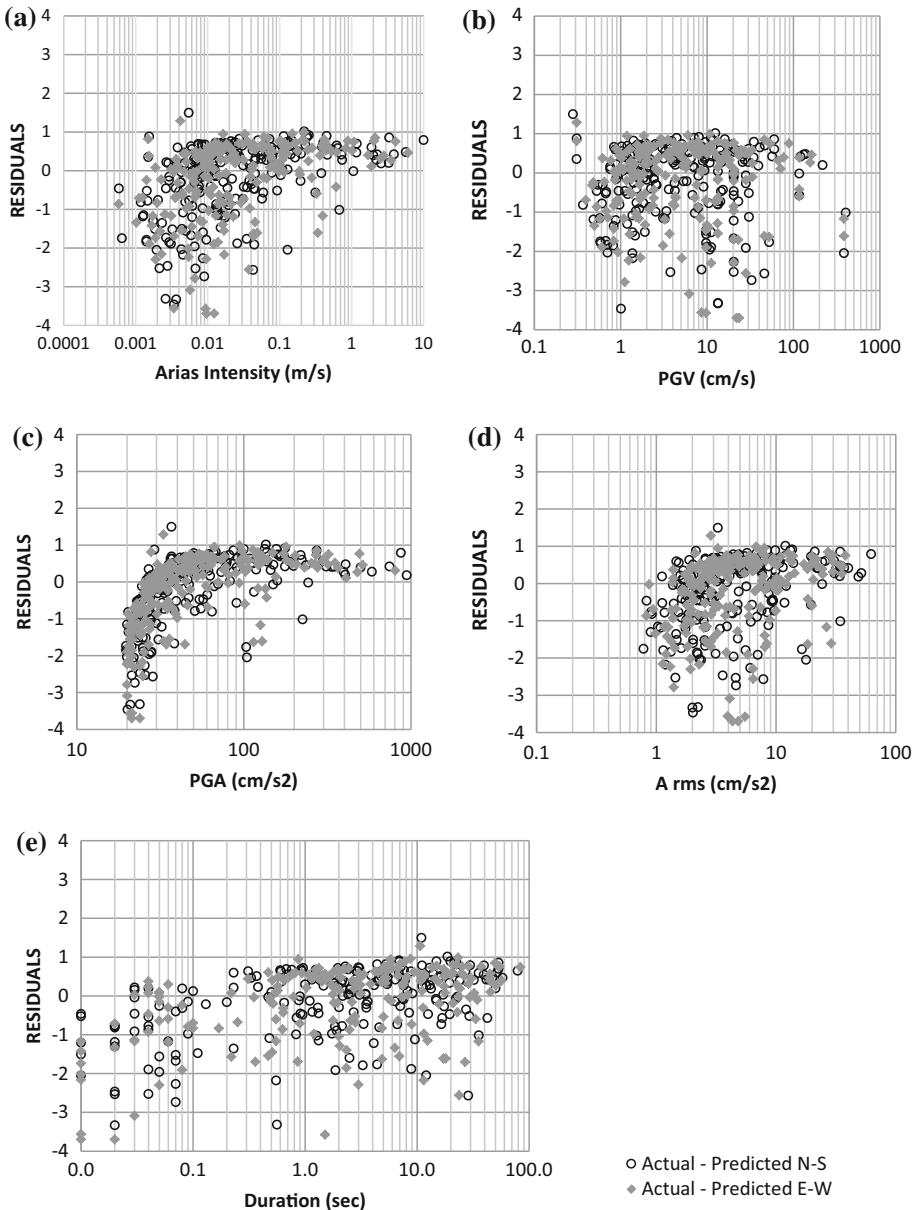


Fig. 9 Residuals of two-IM vector model (PGV, I_a) of Fotopoulou and Pitilakis (2015) model versus **a** Arias intensity, **b** PGV, **c** PGA, **d** A_{rms} , and **e** duration at $a_y = 0.02$ g

obvious trends in the residuals are visible in Fig. 5a–f, except for a slight underprediction observed at the high ground shaking levels in Fig. 5a, b, d. However, a constant shift along the zero line is noticeable in all of these plots indicating that the constant term of the model (a_1 in Eq. 4) should be modified based on the Turkish dataset. Same plots are presented in Fig. 6 for the three-IM vector-valued model with respect to the same ground motion

parameters: I_a , PGA, PGV, A_{RMS} , k_y/PGA and duration in Fig. 6a–f, respectively. When compared to Figs. 5, 6 clearly shows that the inclusion of the third-IM significantly improved the performance of the model. No obvious trends in the residuals and no constant shift along the zero line are observed in Fig. 6. Therefore, three-IM vector-valued model proposed by Saygılı and Rathje (2008) is preferable for PSHA applications in Turkey, even if it increases the computing time significantly by introducing the third IM.

Distribution of the residuals for the NSB displacement prediction model proposed by Bozbey and Gündoğdu (2011) are plotted for with respect to I_a , PGA, PGV, A_{RMS} , k_y/a_{max} and duration in Fig. 7a–f, respectively. Figure 7b, e shows that the model has a constant shift from the actual data points for the parameters included in the model (k_y/a_{max} or PGA). One possible reason for that constant shift might be the difference between the datasets: Bozbey and Gündoğdu (2011) used moderate-to-large magnitude events ($M_w > 5$) to develop the prediction model, whereas more than half of the data used in this study was recorded during $M_w < 5$ earthquakes. As Fig. 7a, c, d, f indicate, proposed model is unable to capture the ground motion properties represented by I_a , A_{RMS} , PGV or duration and any one of those parameters might be included in the predictive model for better performance.

Residuals of the Hsieh and Lee (2011) NSB displacement model with respect to I_a , PGA, PGV, A_{RMS} , and duration are given in Fig. 8a–e, respectively. This model includes one ground motion IM (I_a); however, a significant trend in the residual plots with respect to I_a is still observed, especially in low ground shaking levels (Fig. 8a). Additionally, trends are visible in Fig. 8b through e which indicates that model is unable to capture the ground motion properties represented by the PGA, PGV, A_{RMS} , or duration and any one of those parameters might be included in the predictive model.

Performance of Fotopoulou and Pitilakis (2015) model in predicting the calculated NSB displacements of the ground motions in the Turkish strong ground motion dataset is evaluated by plotting the residuals with respect to: I_a and PGV (included in the model), PGA, A_{RMS} and duration (not included in the model) in Fig. 9a–e, respectively. Observed trends are weak in all figures except for Fig. 9c showing that the model covers the ground motion characteristics represented by PGV, I_a , A_{RMS} , and duration. On the other hand, the trend of the residuals with respect to PGA is very significant and the model's performance in predicting the calculated NSB displacements would have been better if PGA was added as the third-IM. It is noteworthy that the Fotopoulou and Pitilakis (2015) model was developed based on the results of two-dimensional stress–strain deformation analysis, not using the displacements calculated by the NSB analogy. Thus, the observed trends in the residuals could be related to the different modeling approaches used in estimating the displacements.

Figures 2, 3, 4, 5, 6, 7, 8 and 9 show that the NSB displacement prediction models which include more than one IM have smaller bias in estimating the calculated NSB displacements of the Turkish ground motion dataset. PGA is an *efficient*, and *hazard compatible* (as defined by Luco and Cornell 2007) IM and it significantly improves the performance of the prediction model by capturing the high frequency characteristics of the ground motions. However, functional form of the PGA term has a substantial effect on the results. Even if the a_y/a_{max} term is generally preferred, an additional PGA term decreases the bias in the model predictions as observed in Saygılı and Rathje (2008) model. Trends in the residuals are less visible for PGV in the models that include this IM, showing that: (1) PGV is less sensitive to the regional ground motion characteristics when compared to PGA and I_a and (2) the ground motion IMs that reflects the low frequency characteristics such as PGV or S_a at $T = 1$ s significantly reduces the variability and the standard deviation of the model.

Addition of I_a or a similar ground motion parameter such as A_{RMS} to the prediction model generally improves the model performance (with the exception of Hsieh and Lee 2011 model) because I_a is an *efficient* IM for predicting NSB displacement. Since the hazard maps for PGV and I_a are not currently available for Turkey, both of these IMs are not as *feasible* as PGA in regional context. The models derived based on larger datasets with the help of scaled recordings (Watson-lamprey and Abrahamson (2006), Jibson (2007) and Saygılı and Rathje (2008)) are statistically more stable.

4 Vector-valued PSHA for estimating the NSB displacement

In the context of performance-based earthquake engineering (Stewart et al. 2002), the NSB displacement can be considered as an engineering demand parameter (EDP) that describes the performance of slopes. In the PSHA framework, the NSB displacement (D_n) can be computed for several test NSB displacement levels, resulting in a NSB displacement hazard curve that describes the annual rate of exceedance for test displacement levels. The hazard integral for NSB displacement hazard analysis is similar to the traditional hazard integral if only one ground motion IM is employed by the NSB displacement prediction model. For a NSB displacement prediction model that depends on only one-IM, the hazard integral can be written as:

$$\lambda(D_n > z) = \lambda_o \times \int_M \int_R \int_\epsilon P[D_n > z | D_n(IM(M, R, \epsilon), \sigma_{InD})] f_M(M) f_R(M, R) f_\epsilon(\epsilon) \times dM \times dR \times d\epsilon \tag{10}$$

where $D_n(IM(M, R, \epsilon))$ is the median NSB displacement for the given intensity measure and σ_{InD} is the standard deviation of the NSB displacement prediction model. When the NSB displacement model includes more than one IM, the vector hazard integral (Bazzurro and Cornell 2002) is required. For Saygılı and Rathje (2008) prediction model, the NSB displacement hazard integral becomes:

$$\begin{aligned} \lambda(D_n > z) = & \lambda_o \int_M \int_R \int_{\epsilon_{PGA}} \int_{\epsilon_{PGV}} \int_{\epsilon_{I_a}} P[> z | D_n(PGA(M, R, \epsilon_{PGA}), \\ & \times PGV(M, R, \epsilon_{PGV}), I_a(M, R, \epsilon_{I_a}), \sigma_{InD})] \\ & \times f_M(M) f_R(M, R) f_{\epsilon_{PGA}}(\epsilon_{PGA}) f_{\epsilon_{PGV}}(\epsilon_{PGV} | \epsilon_{PGA}) f_{\epsilon_{I_a}}(\epsilon_{I_a} | \epsilon_{PGV}) \\ & \times dM \times dR \times d\epsilon_{PGA} \times d\epsilon_{PGV} \times d\epsilon_{I_a} \end{aligned} \tag{11}$$

In Eqs. (10) and (11); λ_o is the activity rate, M is moment magnitude, R is the distance, ϵ_{PGA} is the number of standard deviations for PGA, ϵ_{PGV} is the number of standard deviations for PGV, ϵ_{I_a} is the number of standard deviations for I_a , $f_{\epsilon_{PGA}}(\epsilon_{PGA})$ is the probability density function (PDF) for ϵ_{PGA} , $f_{\epsilon_{PGV}}(\epsilon_{PGV} | \epsilon_{PGA})$ is the PDF for ϵ_{PGV} conditioned on ϵ_{PGA} , and $f_{\epsilon_{I_a}}(\epsilon_{I_a} | \epsilon_{PGV})$ is the PDF for ϵ_{I_a} conditioned on ϵ_{PGV} . The form of Eq. (11) differs from the formulation given by Bazzurro and Cornell (2002) such that the integral in the equation is over the epsilon values (ϵ_{PGA} , ϵ_{PGV} and ϵ_{I_a}) rather than ground motion parameters (PGA, PGV, and I_a). While mathematically equivalent, this equation clearly shows how the correlation of the variability of the ground motion values should be considered. The PDF of epsilon for the first IM, $f_{\epsilon_{PGA}}(\epsilon_{PGA})$, is given by the standard normal distribution. However, the PDF of epsilon for the second IM, $f_{\epsilon_{PGV}}(\epsilon_{PGV} | \epsilon_{PGA})$, is

conditioned on the ε_{PGA} value and includes the correlation of ε_{PGA} and ε_{PGV} , and so does the PDF of $f_{\varepsilon_{\text{I}_a}}(\varepsilon_{\text{I}_a}|\varepsilon_{\text{PGV}})$. The ε_{PGV} can be defined as a function of ε_{PGA} as:

$$\varepsilon_{\text{PGV}} = \rho_{\text{PGV}|\text{PGA}} \times \varepsilon_{\text{PGA}} \pm \sigma_{\text{PGV}|\text{PGA}} \quad (12)$$

Similarly, the ε_{I_a} can be defined as a function of ε_{PGV} as:

$$\varepsilon_{\text{I}_a} = \rho_{\text{I}_a|\text{PGV}} \times \varepsilon_{\text{PGV}} \pm \sigma_{\text{I}_a|\text{PGV}} \quad (13)$$

where $\rho_{\text{PGV}|\text{PGA}}$ is the correlation coefficient between PGA and PGV, $\rho_{\text{I}_a|\text{PGV}}$ is the correlation coefficient between PGV and I_a , $\sigma_{\text{PGV}|\text{PGA}}$ and $\sigma_{\text{I}_a|\text{PGV}}$ are the standard deviations for these correlations. Parameters of Eqs. (12) and (13) should be computed from the correlation of normalized residuals of the ground motion prediction model. Since the computing time for the vector-hazard integral (Eq. 11) is very long, we have employed only one GMPE, the Abrahamson and Silva (2008) model for estimating the PGA and PGV and one GMPE, the Travarasou et al. (2003) model for estimating I_a in PSHA analysis. The correlation coefficient between PGA and PGV ($\rho_{\text{PGV}|\text{PGA}}$) and its standard deviation ($\sigma_{\text{PGV}|\text{PGA}}$) is calculated using the intra-event residuals of Abrahamson and Silva (2008) model as 0.74 and 0.51. The correlation coefficient between PGV and I_a could not be calculated since the intra-event residuals of the Travarasou et al. (2003) model is not available. The value given by Rathje and Saygılı (2008) for the covariance of Travarasou et al. (2003) and Boore and Atkinson (2007) models (0.64) is directly adopted since the correlation coefficient has a weak dependence on the selected GMPE and the ground motion database (Baker and Cornell 2006). $\sigma_{\text{I}_a|\text{PGV}}$ is assumed to be equal to $\sigma_{\text{PGV}|\text{PGA}}$. Numerical integration of the PSHA integral shown in Eq. (11) is performed by the computer code HAZ39 which was developed by N. Abrahamson for scalar PSHA (PG&E 2010), modified to perform vector-valued PSHA by Gülerce and Abrahamson (2010), and subjected to further modification to perform three-vector PSHA for this study.

5 Hazard curves for the NSB displacement

Vector-valued probabilistic NSB displacement hazard analyses are performed for selected locations in the Bolu-Gerede Region as shown in Fig. 10. Bolu-Gerede Region is located in northwestern Turkey and were subjected to large magnitude earthquakes occurred on the North Anatolian Fault Zone (NAFZ) in 1944 (Bolu-Gerede Earthquake, $M_w = 7.2$), 1967 (Mudurnu Earthquake, $M_w = 6.7$) and 1999 (Düzce Earthquake, $M_w = 7.1$). Gülerce and Ocak (2013) developed planar seismic source characterization (SSC) models that cover the rupture zones of 1967 and 1999 earthquakes. The SSC model for the rupture zone of 1944 Bolu-Gerede Earthquake was provided in Levendoğlu (2013) and Vakilinezhad et al. (2013). These SSC models define planar fault segments for each rupture zone where the geometry of the sub-segments (length, width, and segmentation points) were determined and incorporated with the help of available fault maps. Composite magnitude distribution model (Youngs and Coppersmith 1985) was used for all rupture sources to properly represent the characteristic behavior of NAFZ without an additional background source zone. Fault segments, rupture sources, rupture scenarios and fault rupture models were determined using the Working Group of California Earthquake Probabilities (WGCEP 2003) terminology. Events in the earthquake catalogue (Kalafat et al. 2011) were attributed to the individual seismic sources and scenario weights were determined by balancing the

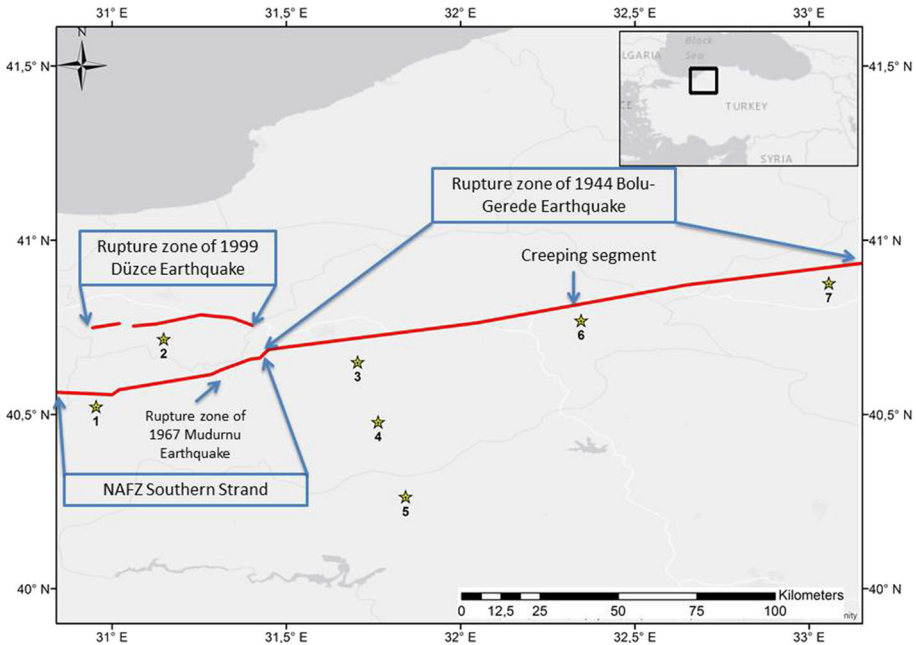


Fig. 10 The general layout of the sites where the PSHA analyses are performed (sites are shown by yellow stars). The simplified segments of the NAFZ included in the SSC model developed by Gülerce and Ocak (2013) and Levendoğlu (2013) are shown by red lines

accumulated seismic energy (based on the annual slip rate) by the released seismic moment for each fault rupture model. Uncertainties involved in each parameter, especially the annual slip rate, annual creep rate, fault widths, b-value, and scenario weights were considered in the logic tree. Sites 3, 6, and 7 are arbitrarily chosen sites with the rupture distance of 5 km at the south of the 1944 Bolu-Gerede Earthquake rupture zone, since some earthquake-induced landslides were observed on the south of the fault plane in this region (R. Ulusay, personal communication). Site 6 is located close to the creeping segment of 1944 earthquake rupture zone to evaluate the effect of slip rate accumulation on the NSB displacement hazard. Sites 4 and 5 are parallel to Site 3, but further away from the fault ($R_{rup} = 25$ km and $R_{rup} = 50$ km, respectively). Site 1 and Site 2 are located close to the other seismic sources in the area: Site 1 is 5 km away from the Southern Strand of NAFZ and Site 2 is 5 km away from the rupture zone of 1999 Düzce Earthquake.

Figure 11a compares the NSB displacement hazard curves for Sites 1, 2, 3, 6, and 7 for rock site conditions ($V_{s30} = 760$ m/s) for the yield acceleration of 0.1 g. Horizontal lines in Fig. 11 show the acceptable hazard levels in building codes; 10% chance of exceedance in 50 years (denoted by the black dashed line) and 2% chance of exceedance in 50 years (denoted by the black solid line). Since all of these sites are 5 km away from the rupture plane, the NSB displacement hazard curves are very close to each other, especially for smaller hazard levels. The estimated NSB displacements at 10% probability of exceedance in 50 years vary between 9 cm for Site 2 (where annual slip rate is smaller since it is shared by parallel fault segments) and 15 cm for Site 7. The NSB displacement estimated for Site 6 is smaller than the others for higher hazard levels since that site is close to the creeping segment of NAFZ and the annual slip rate of this segment is approximately 40% smaller

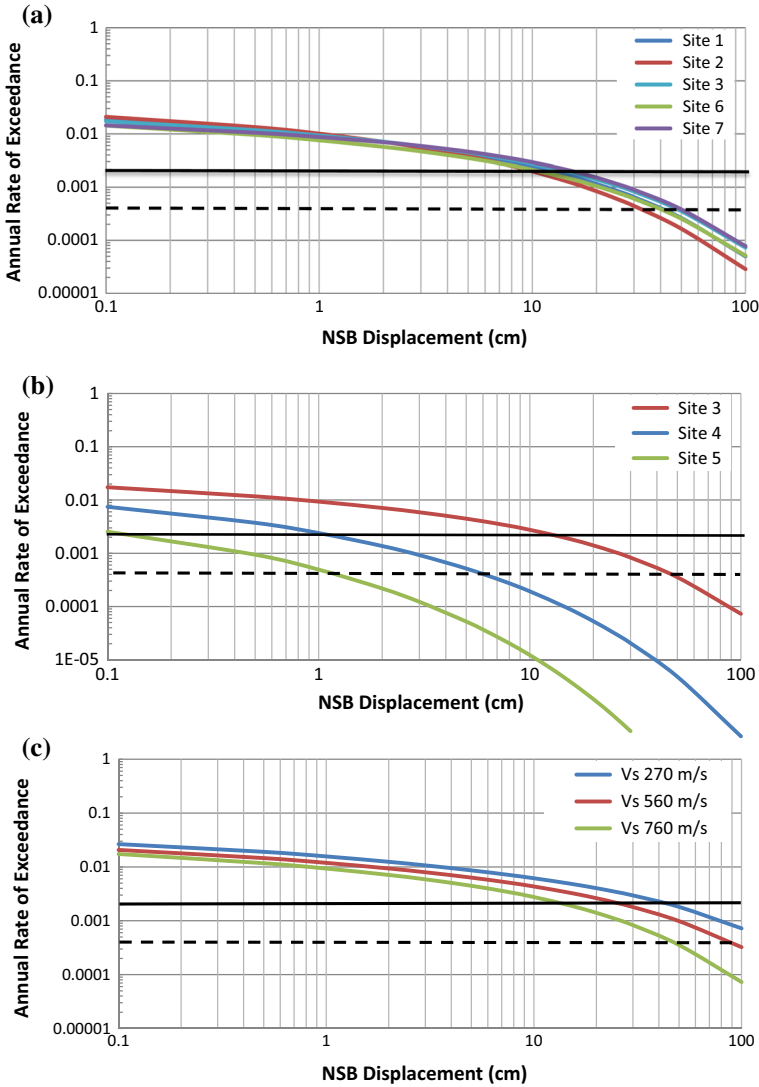


Fig. 11 **a** Comparison of the NSB displacement hazard curves for Sites 1, 2, 3, 6 and 7, **b** comparison of the NSB displacement hazard curves for Sites 3, 4 and 5, **c** NSB displacement hazard curves for different average shear wave velocities at the top 30 m for Site 3

than the neighboring segments. NSB displacement hazard at Sites 3 and 7 are larger than the other sites, since they are in the near vicinity of the longest segments of the whole system with the highest characteristic magnitudes (M_{char}). The NSB displacements for 2% probability of exceedance in 50 years (32–48 cm) are significantly higher than 475-year return period estimates for the same sites.

The NSB displacement hazard curves for Site 3, Site 4 and Site 5, which are located 5, 25 and 50 km away from the nearest segments, are presented in Fig. 11b. The range of variation in estimated NSB displacement based on the distance to the fault plane is

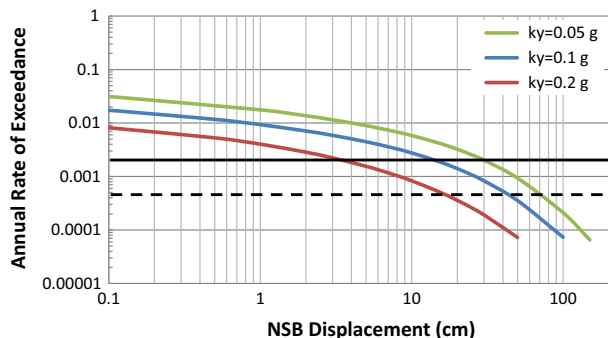
substantial. For rock site conditions ($V_{S30} = 760$ m/s) and with the yield acceleration value of 0.1 g, the 475-years return period NSB displacement is 14 cm for Site 3, 1 cm for Site 4, and even below 1 cm for Site 5. The 2475-year return period NSB displacements are 48 cm for nearest site (Site 3) and about 1 cm in the far-field (Site 5). These results clearly show that the earthquake induced landslide hazard is critical for near fault zones, however, the effect diminishes away quickly as the rupture distance increases. The effect of local site conditions on the NSB displacement hazard curves is shown in Fig. 11c. Different average shear wave velocity values at the top 30 m are chosen according to the NEHRP (1997) site class definitions to represent rock site conditions ($V_{S30} = 760$ m/s), soft rock (or very dense soil) conditions ($V_{S30} = 560$ m/s), and soil site conditions ($V_{S30} = 270$ m/s). The 475-years return period NSB displacement value increases as the V_{S30} value decreases: NSB displacement is about 14 cm for rock, 25 cm for soft rock, and 42 cm for soil site conditions. Similarly the NSB displacement for 2% probability of exceedance in 50 years is estimated as 48 cm for rock, 88 cm for soft rock, and greater than 100 cm for soil site conditions. According to the NSB analogy, slope tends to deform as a single massive block which means a rigid-perfectly plastic stress–strain behavior on a planar failure surface; therefore, high V_{S30} values are more relevant with NSB displacement hazard analysis.

The yield acceleration value has a considerable effect on the resulting NSB displacement. In Fig. 12, the NSB displacement hazard curves at Site 3 for different yield acceleration values are compared. The NSB displacement for 10% probability of exceedance in 50 years is about 2 cm for yield acceleration of 0.2 g, but this value increases significantly with decreasing yield acceleration. 14 cm NSB displacement is computed for the yield acceleration of 0.1 g, and 28 cm is computed for yield acceleration of 0.05 g at the same hazard level. For 2% probability of exceedance in 50 years, the NSB displacement values are 18 cm for yield acceleration of 0.2 g, 48 cm for yield acceleration of 0.1 g, and 75 cm for yield acceleration of 0.05 g.

6 Summary and conclusions

The primary objective of the study is to test the compatibility of the candidate NSB displacement prediction models with calculated NSB displacements in the Turkish strong motion dataset. Analysis results showed that the performance of three-IM NSB displacement prediction model proposed by Saygılı and Rathje (2008) is superior in predicting the calculated NSB displacements in the Turkish ground motion dataset without any systemic

Fig. 12 NSB displacement hazard curves for different yield acceleration values at Site 3



bias. Even though many NSB displacement prediction models based on local and global strong motion datasets were proposed in the past ten years, these models were not incorporated into the PSHA software and combined by planar seismic source characterization models developed for active tectonic regions, except for a few examples in United States. In this study, three-IM vector-valued NSB displacement prediction model of Saygılı and Rathje (2008) is incorporated into the vector-valued PSHA integral and the NSB displacement hazard curves for different site conditions and yield acceleration levels are developed.

Evaluation of the NSB displacement hazard curves showed that the distance to the fault plane is the most important factor for quantifying the hazard for seismically induced landslides. NSB displacements estimated in the close vicinity of the fault plane (especially up to 5 km) are significantly higher than the estimated NSB displacements for the far field sites. Parameters of the SSC model such as the annual slip rate and the maximum magnitude (M_{\max}) have a considerable effect on the NSB displacement hazard curve. The sites located near the segments of the NAFZ with lower slip rate are less prone to the NSB displacement hazard when compared to the sites with equal rupture distances. As the V_{S30} of the site decreases from 760 to 270 m/s (keeping in mind that NSB displacement analogy is more appropriate for rock sites), estimated NSB displacement increases significantly; therefore, the soft rocks classified as Class C according to NEHRP (1997) are subjected to larger NSB displacement hazard than the Class B sites. The underlying reason for this increase is the linear and nonlinear site amplification models included in the GMPEs; therefore, this effect becomes more substantial in the higher hazard levels.

To apply the method summarized here in engineering applications, shortcomings of this framework should be carefully considered. Yield acceleration value has a significant effect on the NSB displacement hazard curves. Current practice (e.g. HAZUS 2012) uses several geological-geomorphological factors such as slope angle, groundwater conditions, etc. to estimate the yield accelerations. In addition to these factors, geotechnical tests results should be considered in site-specific applications to properly estimate the yield acceleration. It is notable that the damage measures for the NSB displacement are not clearly defined. Current applications only provide the annual rates of exceeding certain NSB displacement values but do not state the limiting values for the failure of the slope or any other performance objective. Damage measures for the NSB displacement values may be determined by comparing these results with the case histories. However, the NSB analogy is only valid for soils that can behave as a rigid block and many documented earthquake induced landslides are not suitable for NSB analysis. An example for the validation procedure of the method defined here for the Bakacak Landslide observed during 1999 Düzce Earthquake and the discussion of the limitations is provided in Balal and Gülerce (2015).

This study intends to provide the roadmap for the PSHA for estimating the earthquake induced landslides. However, parameters that reflect the site conditions in this framework are limited to V_{S30} and yield acceleration. Using the method documented here, a fully-probabilistic framework for estimating the earthquake-induced landslide hazard including the landslide susceptibility parameters (topography, groundwater, settlement, vegetation etc.) may be developed. Compatibility of Abrahamson and Silva (2008) model and all other NGA-W1 horizontal models is discussed thoroughly in Gülerce et al. (2016). On the other hand, applicability of the Arias intensity prediction models to Turkey needs to be evaluated within the proposed framework.

Acknowledgements “Earthquake-induced Landslide Risk in Western Black Sea Region” Project was supported by METU (BAP Award Number: BAP-08-11-2013-001). We are thankful to Prof. Dr. Reşat Ulusay for fruitful discussions regarding the earthquake induced landslides inventory of Turkey. The authors wish to acknowledge Dr. Fuat Şaroğlu for his contribution on seismic source models for NAFZ Bolu-Gerede Segment. We appreciate the help and support of Norman A. Abrahamson regarding the PSHA code. Figure 1c and 9 are prepared with the help of Burak Akbaş, which is greatly appreciated. We are grateful for the constructive comments provided by the anonymous reviewers.

References

- Abrahamson NA, Silva WJ (2008) Summary of the Abrahamson & Silva NGA ground-motion relations. *Earthq Spectra* 24(1):67–97
- Akkar S, Çağnan Z, Yenier E, Erdoğan Ö, Sandıkkaya A, Gülkan P (2010) The recently compiled Turkish strong motion database: preliminary investigation for seismological parameters. *J Seismol* 14:457–479
- Ambraseys NN, Menu JM (1988) Earthquake-induced ground displacements. *Earthq Eng Struct Dyn* 16:985–1006
- Ambraseys NN, Srbulov M (1994) Attenuation of earthquake-induced displacements. *Earthq Eng Struct Dyn* 23:467–487
- Ambraseys NN, Srbulov M (1995) Earthquake induced displacements of slope. *Soil Dyn Earthq Eng* 14:59–71
- Baker JW, Cornell CA (2006) Correlation of response spectral values for multicomponent ground motions. *Bull Seismol Soc Am* 96(1):215–227
- Balal O, Gülerce Z (2015) Probabilistic seismic hazard assessment of seismically induced landslide for Bakacak-Düzce region. *Eng Geol Soc Territ* 2:681–684
- Bazzurro P, Cornell CA (2002) Vector-valued probabilistic seismic hazard analysis (VPSHA). In: Proceedings of 7th U.S. national conference on earthquake engineering, paper #61, Boston, Massachusetts
- Boore DN, Atkinson G (2007) Boore-Atkinson NGA ground motion relations for the geometric mean horizontal component of peak and spectral ground motion parameters, PEER Rep. 2007/01, Pacific Earthquake Engineering Research Center, University of California, Berkeley
- Bozbey İ, Gündoğdu O (2011) A methodology to select seismic coefficients based on upper bound “Newmark” displacements using earthquake records from Turkey. *Soil Dyn Earthq Eng* 31:440–451
- Bradley BA (2013) A New Zealand-Specific pseudospectral acceleration ground-motion prediction equation for active shallow crustal earthquakes based on foreign models. *Bull Seismol Soc Am* 103:1801–1822
- Bray JD, Travararou T (2007) Simplified procedure for estimating earthquake-induced deviatoric slope displacements. *J Geotech Geoenviron Eng* 133(4):381–392
- Chiou B, Darragh R, Gregor N, Silva W (2008) NGA project strong motion database. *Earthq Spectra* 24:23–44
- Crespellani T, Madiari C, Vannucchi G (1998) Earthquake destructiveness potential factor and slope stability. *Geotechnique* 48(3):411–419
- Fotopoulou SD, Pitalakis KD (2015) Predictive relationships for seismically induced slope displacements using numerical analysis results. *Bull Earthq Eng* 13:3207–3238
- Gülerce Z, Abrahamson NA (2010) Vector-valued probabilistic seismic hazard assessment for the effects of vertical ground motions on the seismic response of highway bridges. *Earthq Spectra* 26(4):999–1016
- Gülerce Z, Ocak S (2013) Probabilistic seismic hazard assessment of Eastern Marmara Region. *Bull Earthq Eng* 11(5):1259–1277
- Gülerce Z, Kargıoğlu B, Abrahamson NA (2016) Turkey-adjusted NGA-W1 horizontal ground motion prediction models. *Earthq Spectra* 32(1):1–25
- Hazus MH 2.1 (2012) Multi-hazard loss estimation methodology earthquake model technical manual. Department of Homeland Security Federal Emergency Management Agency Mitigation Division Washington, D.C.
- Hsieh S, Lee C (2011) Empirical estimation of the Newmark displacement from the Arias intensity and critical acceleration. *Eng Geol* 122:34–42
- Jibson RW (1993) Predicting earthquake-induced landslide displacements using Newmark’s sliding block analysis. *Transp Res Rec* 1411:9–17
- Jibson RW (2007) Regression models for estimating coseismic landslide displacement. *Eng Geol* 91:209–218
- Jibson RW, Harp EL, Michael JM (1998) A method for producing digital probabilistic seismic landslide hazard maps: an example from the Los Angeles, California area. US Geological Survey Open-File Report, pp 98–113

- Kalafat D, Güneş Y, Kara M, Deniz P, Kekovali K, Kuleli HS, Gülen L, Yilmazer M, Özel NM (2011) A revised and extended earthquake catalogue for Turkey since 1900 ($M \geq 4.0$). Boğaziçi University, Kandilli Observatory and Earthquake Research Institute Report
- Levendoğlu M (2013) Probabilistic seismic hazard assessment of Ilgaz-Abant segments of North Anatolian fault using improved seismic source models, MS Thesis Dissertation, Middle East Technical University
- Luco N, Cornell CA (2007) Structure-specific scalar intensity measures for near-source and ordinary earthquake ground motions. *Earthq Spectra* 23(2):357–392
- Newmark NM (1965) Effects of earthquakes on dams and embankments. *Geotechnique* 15(2):139–160
- Pacific Gas and Electric Company (2010) Verification of PSHA Code Haz43. GEO.DCPP.10.03 Rev 0
- Rathje EM, Saygılı G (2008) Probabilistic seismic hazard analysis for the sliding displacement of slopes: scalar and vector approaches. *J Geotech Geoenviron Eng* 134(6):804–814
- Saygılı G, Rathje EM (2008) Empirical predictive models for earthquake-induced sliding displacements of slopes. *J Geotech Geoenviron Eng* 134(6):790–803
- Saygılı G, Rathje EM (2009) Probabilistically based seismic landslide hazard maps: an application in Southern California. *Eng Geol* 109:183–194
- Scasserra G, Stewart JP, Bazzurro P, Lanzo G, Mollaioli F (2009) A comparison of NGA ground-motion prediction equations to Italian data. *Bull Seismol Soc Am* 99:2961–2978
- Shoja-Taheri J, Naserieh S, Hadi G (2010) A test of the applicability of NGA models to the strong ground-motion data in the Iranian plateau. *J Earthqu Eng* 14:278–292
- Stafford PJ, Strasser O, Bommer JJ (2008) An evaluation of the applicability of the NGA models to ground-motion prediction in the Euro-Mediterranean region. *Bull Earthq Eng* 6:149–177
- Stewart JP, Chiou S-J, Bray JD, Graves RW, Somerville PG, Abrahamson NA (2002) Ground motion evaluation procedures for performance-based design. *Soil Dyn Earthq Eng* 22(9):765–772
- Süzen ML, Doyuran V (2004) Data driven bivariate landslide susceptibility assessment using geographical information systems: a method and application to Asarsuyu catchment, Turkey. *Eng Geol* 71:303–321
- Tothong P, Cornell CA (2006) An empirical ground-motion attenuation relation for inelastic spectral displacement. *Bull Seismol Soc Am* 96(6):2146–2164
- Travasarou T, Bray JD, Abrahamson NA (2003) Empirical attenuation relationship for Arias intensity. *Earthq Eng Struct Dyn* 32:1133–1155
- Vakilinezhad M, Levendoğlu M, Gülerce Z, Şaroğlu F (2013) Effect of fault characteristics on the probabilistic seismic hazard assessment results. In: Proceedings of international conference on earthquake engineering, 29–31 May 2013, Skopje
- Wang Y, Rathje EM (2015) Probabilistic seismic landslide hazard maps including epistemic uncertainty. *Eng Geol* 196:313–324
- Watson-Lamprey J, Abrahamson NA (2006) Selection of ground motion time series and limits on scaling. *Soil Dyn Earthq Eng* 26(5):477–482
- Working Group on California Earthquake Probabilities (2003) Earthquake probabilities in the San Francisco Bay Region: 2002–2031, U.S. Geological Society Open File, Report 03–214
- Yegian MK, Marciano EA, Ghahraman VG (1991) Earthquake induced permanent deformations: probabilistic approach. *J Geotech Eng* 117:35–50
- Youngs RR, Coppersmith KJ (1985) Implications of fault slip rates and earthquake recurrence models to probabilistic seismic hazard estimates. *Bull Seismol Soc Am* 75:939–964